Seasonal sediment dynamics on the Barcelona inner shelf (NW Mediterranean): A small Mediterranean river- and wave-dominated system

L. López[a,*], J. Guillén[a], A. Palanques[a], M. Grifoll[b]

[a] Department of Marine Geosciences, Institut de Ciències del Mar (CSIC), Passeig Marítim de la Barceloneta 37–49, 08003, Barcelona, Spain
[b] Department of Civil and Environmental Engineering, BarcelonaTech (UPC), c./Jordi Girona, 1–3, 08034 Barcelona, Spain

Abstract

The seasonal pattern of sediment dynamics on an inner shelf characterized by the presence of sediment delivered by a small, mountainous river (with a “flash-flood” regime) was investigated. Near-bottom suspended sediment fluxes across the shelf (i.e. 20, 30 and 40 m water depth) were estimated using observations from three benthic tripods deployed from September 2007 to June 2008. Near-bottom sediment resuspension is controlled by wave-induced currents and river-born sediment availability, whereas the shelf currents play a secondary role. Fourteen sediment transport events were identified (eight in autumn, two in winter and four in spring), with transport rates according to storm intensity and sediment availability. These few energetic events induced a large percentage of the cumulative sediment transport near the bottom. However, the lack of proportionality between suspended sediment transport rates and the combined wave-current bottom shear stress in some events highlights the importance of the sequence of events in sediment dynamics. Since wave activity, hydrography and river discharges display a strong seasonal pattern in the NW Mediterranean, the resulting sediment dynamics across the shelf also correspond to a seasonal cycle. This seasonal variability leads to a temporal evolution of the bottom grain size (coarser in winter) and the near-bottom sediment transport rates (higher in spring and autumn) which is consistent with the seasonal pattern of the hydrodynamic events and the river discharge load.

Keywords: Sediment resuspension; sediment transport events; river-born sediment availability; flash-flood regime; mountainous river; Besòs River.

---

[*] *Corresponding author. Tel.: +34 932 309 600; Fax: +34 932 309 555. E-mail: (L.López).*

1. Introduction

The influence of river floods and storms on sediment delivery and reworking has been recognized in many recent studies of river-dominated continental shelves, where river inputs and storm waves have been found to be the dominant forcing mechanisms of sediment dynamics (e.g. Cacchione et al., 1995; Ogston and Stemberg, 1999; Sherwood et al., 1994). In small-river systems (drainage basins <10^4 km^2), where most of the annual sediment load is discharged during episodic events, the short duration of floods can lead synoptic-scale (days to weeks) meteorological forcing to have a more important role in the fate of the sediment discharged onto the continental shelf (Bever et al., 2011; Geyer et al., 2000). Discharged sediment from small-river floods can remain close to the river mouth on shelves with micro-tidal conditions and moderate significant wave heights. In these cases, sediments that are deposited nearshore can be subsequently resuspended and transported to distal portions of the system when shear stresses become sufficiently high (Grifoll et al., 2014; Guillén et al., 2006). The suspended load is then the main sediment transport mechanism resulting in sediment winnowing and erosion across the shelf (Allison et al. 2000; Grifoll et al., 2013_1).

The NW Mediterranean Sea is a micro-tidal and low-energy system from the wave climate perspective. Floods and storm-generated wave effects on coastal sediment resuspension and transport on the shelf have been emphasized by several studies on the Ebro continental shelf (Guillén et al., 2002; Jiménez et al., 1999; Palanques et al., 2002; Puig et al., 2001) and on other shelves of the northwestern Mediterranean (Dufois et al., 2014; Ferré et al., 2005; Guillén et al., 2006; Palanques et al., 2011; Roussiez et al., 2005; Ulses et al., 2008). These investigations revealed that wave-induced bottom shear stress is generally the main stirring factor for sediment resuspension and transport and is mainly effective in the inner shelf region. However, strong storm waves could also resuspend fine-grained sediments from the mid-shelf and transport them off-shelf (Puig et al., 2001; Simarro et al., 2015). The along-shelf sediment fluxes are dominant during most of the time on NW Mediterranean continental shelves (Grifoll et al., 2013_1; Palanques et al., 2002), although it has been reported that extreme floods and storms in the Gulf of Lions can lead to across- and along-shelf sediment transport of about the same order of magnitude (Bourrin et al., 2008; Palanques et al., 2011; Ulses et al., 2008). The resulting surface sediment distribution and the location of the prodeltaic mud deposits have been observed to be coherent with the hydrodynamic processes and induced near-bottom sediment fluxes. The finest sediment accumulates mainly on the mid-shelf, where the lowest mean combined wave-current shear stresses occur, whereas on the inner shelf some mud accumulates but is frequently resuspended due to the high combined wave-current shear stresses occurring in this region (Grifoll et al., 2014; Palanques et al., 2002).

As yet, few studies have addressed sediment dynamics on continental shelves off a “small” Mediterranean river system (e.g. the Têt River in the Gulf of Lions: Bourrin et al., 2008; Guillén et al., 2006). Guillén et al. (2006) differentiated episodes of sediment dispersal on the inner shelf of the Têt River during “wet storms”, when storm conditions coincide with local precipitation and elevated river discharge, and “dry storms”, when storm waves occur in the absence of significant river discharge. The main differences between the wet and dry storms arose after the storm. This “small” Mediterranean river system allows the deposition of fine-grained particulate material near the river mouth during flood events as ephemeral layers. Their location above the storm wave base make them subjected to regular resuspension events that transport these fine materials further offshore. Further, Bourrin et al. (2008) analysed sediment dynamics from a flood event with a five-year return interval in the Têt River basin and on the adjacent inner shelf of the Gulf of Lions. Their results show that floods with a few-year return interval in small coastal rivers can play a significant role in the transport of sediments on microtidal continental margins and their export from the shelf through canyons. However, no study has been published on seasonal characterization of sediment dynamics in a “small” Mediterranean river system.

The present study investigates sediment dynamics in the shelf and quantifies sediment transport on a micro-tidal inner shelf influenced by a small Mediterranean river, the Besòs River (Barcelona, NW Mediterranean Sea – Figure 1). In particular, this study focuses on the effect of floods and storms on sediment dynamics over a year, emphasizing in the characteristics of the forcing conditions during sediment transport events and their frequency and distribution along the seasons of the year (i.e. the seasonal variability of near-bottom sediment transport).

The paper is organized as follows. Section 2 introduces the study area characteristics and the methods used to obtain the data analysed thereafter. Section 3 includes the analysis of the meteo-oceanographic forcing conditions and the momentum terms in both along- and across-shelf directions; we examine the seasonal variation at a point where water velocity data are available (near-bottom at 20, 30 and 40 m water depth) and the variability of the bottom sediment grain size and seabed level in response to these meteo-oceanographic conditions throughout the study period. Section 4 considers the representativeness of the results, and in particular the way in which sediment dynamics respond to different forcing mechanisms and the role played by stratification. Finally, in Section 5, we present some conclusions on the seasonal sediment dynamics patterns off a small Mediterranean river system obtained from the analysis in Section 4.

2. Methods

Study area

The Besòs River is a short river with a mountainous basin of 1029 km^2 and its main course flows north-south along 52 km from the Catalan Coastal Ranges to the Mediterranean Sea. Its water discharge is variable, with higher values in spring and autumn and minimum values in summer (Liquete et al., 2009; Palanques and Díaz, 1993). Mean water discharge between 1968 and 2008 was 6.8 m^3/s at the gauging station located 2.8 km upstream from the river mouth, where the maximum water discharge of 270 m^3/s was measured on 9 May 1991 (Liquete et al., 2009). The sediment load in the lower part of this river is affected seasonally by relatively intense rains (Palanques, 1994). The sandy sediment developed a small delta plain and the fine sediment developed the prodelta (Checa et al., 1988). The Besòs River annual sediment discharge, averaging 15000 t/year, forms a delta of 8.3 km^2 with a coastal development of 7.6 km shifted southwestwards from the river mouth as a result of the dominant littoral circulation (Liquete et al., 2007).

Statistical analysis of wave conditions in the region from 1984 to 2004 showed a mean significant wave height value (Hs) of 0.70 m, an Hs maximum of 4.61, a maximum wave height of 7.80 m and an averaged mean period of 4.29 s (Gómez et al., 2005). Storms occur mainly from October to April and the most important ones are those coming from the east, due to the combination of the coastal orientation and the Mediterranean climate (Bolaños et al., 2008; Sánchez-Arcilla et al., 2008). The winds are characterized by little inter-annual variability (Cerralbo et al., 2015; Font, 1990). The predominant winds come primarily in autumn and winter from the north and northwest, where their energy is concentrated in low frequencies associated with low-pressure systems, which in this area of the NW Mediterranean Sea corresponds to 3-12 days. In summer and spring, the dominant winds are southwesterly, with the dominant frequencies being the low-pressure systems and diurnal (sea breeze) bands (Cerralbo et al., 2015; Font, 1990). On the inner part of the shelf, the frictional forces tend to prevail, leading to a predominance of depth-averaged along-shelf flows over depth-averaged across-shelf flows; the depth-averaged along-shelf flow variability is driven basically by local wind-forcing and remote sea level gradients, and is influenced by water column stratification and rapid pulses of river discharge (Grifoll et al., 2012; 2013_2). The tidal range is lower than 0.2 m.

The Barcelona continental shelf is a narrow shelf (6–20 km) with the shelf break at 110–120 m depth (ITGE, 1989). The Llobregat and Besòs Rivers provide the main sediment supply, which tends to be transported southwestward due to the action of the dominant along-shelf current (Flexas et al., 2002; Font et al., 1995; Rubio et al., 2005). The monitoring of sediment dynamics in the coastal zone of Barcelona reveals frequent resuspension of bottom sediment caused by waves during storms (Antonijuan et al., 2012; Grifoll et al., 2013_1), and only the finest fractions can be transferred to the slope and beyond through permanent nepheloid layers (Palanques et al., 2008; Puig and Palanques, 1998). The sediment distribution therefore has the same characteristics as other Mediterranean shelves that receive significant discharges from rivers (Liquete et al., 2010; Palanques et al 1990; Palanques and Díaz, 1994; Puig et al., 1999): (1) medium- to well-sorted sand (0.25 mm) in less than 15 to 20 m water depth; (2) mostly silt and clay (0.0078 to 0.0039 mm) distributed to the south from the mouth of the Besòs River between 20 and 60 m depth; and (3) biogenic relict silty sand (0.0625 to 0.125 mm), which covers the shelf from 60 m depth to the continental slope. Liquete et al. (2007) recognized two main morphosedimentary domains: a modern, river-influenced area and a relict, sediment-depleted area. The modern, river-influenced shelf includes the Llobregat and Besòs adjacent prodeltas, which represent the main Holocene depocenter in the area located between 30 and 60 m water depth.

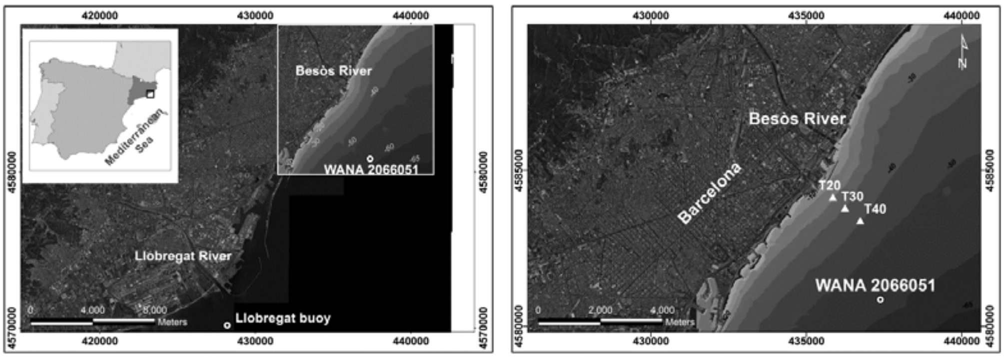

Figure 1. Maps of the Barcelona continental shelf showing the study area and the position of the benthic tripods deployed: T20 at 20 m water depth, T30 at 30 m depth and T40 at 40 m depth. The map projection is UTM zone 31N datum ED50.

Data collection

Three benthic tripods were deployed on the Barcelona continental shelf at 20, 30 and 40 m water depths (Figure 1) during the four SEDMET field cruises carried out from September 2007 to June 2008 aboard the R/V *García del Cid* and the R/V *Sarmiento de Gamboa*. Each tripod was equipped with several sensors and instruments: an Aanderaa Doppler current meter (RCM-9) coupled with a pressure sensor and an Aanderaa optical backscatter

Formatat: anglès (EUA)

Comentari [LL1]: Es demasiado pequeña?
No se apreciaba todo en una figura y he hecho dos y como mejor quedan es de lado pero quizás es muy pequeña!!

turbidimeter placed at 0.53 metres above bottom (mab) and a NKE ALTUS altimeter placed at 0.22 mab. In addition, a set of vertical hydrographic profiles, surficial and near-bottom water samples and bottom sediment samples were obtained along the tripod transect during the deployments. The hydrographic profiles were made using a Sea-Bird SBE 9 CTD coupled with a Seapoint turbidimeter and a set of Niskin bottles. Data collection was carried out in one day in order to obtain a quasi-simultaneous picture of the hydrographic and nepheloid structures. Sediment samples were collected with a small box corer with one acrylic cylindrical core tube (inner diameter = 135 mm) designed to obtain an undisturbed sediment core with a maximum length of 30 cm.

The first deployment was carried out at the beginning of autumn (27–29 September 2007) to define the initial conditions of the system in terms of hydrography and bottom sediment characteristics. The second and third deployments (28–30 November 2007 and 28–29 February 2008, respectively) were scheduled to perform equipment maintenance tasks and to collect representative samples of the bottom sediment and the hydrographic structure of autumn and winter, respectively. Finally, on 19 June 2008 the equipment was recovered and the bottom sediment sampling and hydrographic profiles were performed to characterize the area at the end of the spring season, which corresponded to the end of the study period. The field data recovered in each deployment are listed in Table 1.

FIELD DATA			**SEDMET-I (27/09/07)**	**SEDMET-II (28/11/07)**	**SEDMET-III (28/02/08)**	**SEDMET-IV (19/06/08)**
HYDROGRAPHY		**Hydrographic Profiles**	3	3	3	3
SEDIMENT SAMPLES		**Sediment Cores**	3	3	3	3
TRIPODS	**T20**	**Current Velocity**	DEPLOYMENT	Ok	Ok	Ok
		Pressure		Ok	Ok	Ok
		Turbidity (0-20 NTU range)		Ok	Ok	Ok
		Seabed Level		Failed	Partly	Ok
	T30	**Current Velocity**		Ok	Ok	Partly
		Pressure		Ok	Ok	Partly
		Turbidity (0-20 NTU range)		Ok	Ok	Partly
		Seabed Level		Failed	Partly	Ok
	T40	**Current Velocity**		Ok	Not recovered	Not recovered
		Pressure		Ok		
		Turbidity (0-20 NTU range)		Ok		
		Seabed Level		Failed		

Table 1. Available field data summary during the study period.

Wave measurements from the Llobregat directional buoy were used as wave conditions during the study period. This buoy was located at 45 m water depth (Figure 1) and recorded data every hour. Interruptions in the buoy time series were filled in with data from the WANA model (50 m water depth, Figure 1), which provides directional wave information every three hours. The WANA data have been computed by the Spanish National Institute of Meteorology using the HIRLAM and WAM numerical model since 1991 (Spanish Port Authority). Wave height and period data from the WANA model were calibrated through linear regression using the buoy observations from October 2001 to December 2008 (Sancho-García et al., 2013). Winds were also obtained from the WANA data set and rotated following the orientation of the isobaths (42º) to obtain the across and along components. The Besòs River daily discharge was obtained from the Catalan Water Agency water discharge gauging station located 2.8 km upstream from the Besòs River mouth.

Data processing

Shallow-water effects in the swell: The shoaling and refraction coefficients were calculated to correct wave height as waves move from the 45 m depth (buoy location) to the 20 m, 30 m and 40 m sites, where the instruments were deployed. The shoaling (k_s) and refraction (k_r) coefficients were approximated with a MATLAB function following the manual computation methods taken from WMO (1998):

$$k_s = \frac{H}{H_0} = \sqrt{\frac{C_{g0}}{C_g}} = \sqrt{\frac{1}{2}\frac{C_0}{C_g}}$$

where C_0 is the phase velocity in deep water ($\sqrt{g/k_0}$), k_0 is the wavenumber in deep water and H_0 is the wave height in deep water.

$$k_r = \frac{H}{H_0} = \sqrt{\frac{\cos\alpha_0}{\cos\alpha}}$$

where α_0 is the angle between a wave crest and a local isobath in deep water.

Shear velocities and the total maximum shear stress: A one-dimensional (1D) sediment transport model (Harris and Wiberg, 1997; 2002; Wiberg and Smith, 1983; Wiberg et al., 1994) was used to predict the wave and current near-bottom velocity profiles, values of boundary shear stress and compute suspended sediment concentration, which presented good agreement with the observational data during times of elevated wave shear velocity (data not shown).The model represented the frictional momentum balance in the bottom boundary layer using an eddy viscosity profile enhanced by wave-current interaction. Then, the total shear stress is computed in such a way as to account for differences in direction between the waves and the current:

$$\tau_{cw} = \left[\left(\tau_{cp} + \tau_w\right)^2 + \tau_{cn}^2\right]^{1/2};\ \tau_w = \rho U_{*w}^2,\ \tau_{cp} = \rho U_{*c}^2 \cos\varphi,\ \tau_{cn} = \rho U_{*c}^2 \sin\varphi$$

where, τ_w is the boundary shear stress associated with the waves, τ_{cp} and τ_{cn} are the wave-parallel and wave-normal components of the mean current boundary shear stress, respectively; ρ is the water density; U_{*c} and U_{*w} are the shear velocities for the current and waves, respectively; and φ is the difference in the direction of the waves and the current.

The time series of current velocities measured at 0.53 cm above bottom, wave period and direction and the near-bottom wave-orbital velocity were used as inputs to the model, along with the bed characteristics: the average measured bed sediment size distribution, bed sediment concentration (1 – porosity) and the resuspension parameter (γ_0), based on grain-size and geotechnical analysis. The sediment size distribution represents 6 sediment fractions for the upper centimetre at each location and for each deployment with the corresponding critical shear stress for initiation of motion and settling velocity, estimated using the methodology of Soulsby (1997). The bottom wave-orbital velocity was calculated using the method implemented by Wiberg and Sherwood (2008), which consist in a MATLAB function for calculating the representative bottom orbital velocity (U_{br}) from H_s and T_p using a parametric spectrum.

Calibration of turbidimeters and grain size analysis: Turbidimeters express the light scattering intensity as an equivalent of Formazin turbidity Units (FTU). This calibration was conducted by the manufacturer using Formazin (turbidity calibration standards). In order to convert FTU units into concentration units (mg/L), turbidity sensors were transformed using the measurements obtained by Guillén et al. (2000) from 25 northwestern Mediterranean samples taken in a nearby area. The intensity of the light backscattered by particles was calibrated with a Formazin solution to calculate the suspended sediment concentration (SSC) with the equation:

$$\boldsymbol{SSC(mg/L) = 1.21FTU + 0.43} \qquad (\boldsymbol{r^2 = 0.46})$$

The sediment grain size distribution from the sediment samples was determined by a settling tube for the fraction >50 µm and by a Sedigraph 5100D (Micrometrics) for the fraction <50 µm following the method described by Giró and Maldonado (1985).

Along- and across-shelf currents and near-bottom suspended sediment fluxes: Aanderaa current meters (0.58 mab) output the module of the current intensity and direction measured from the north. These were decomposed to u and v components with positive values towards the N and E, respectively. The along- and across-shelf components were then defined following the orientation of the isobaths (42º for all sites), with positive values towards the NE and offshore, respectively. Assuming that the output of the backscatter sensors was largely attributable to suspended particles and that particles move with the velocity of the water within which they are suspended (Wright, 1995), the instantaneous near-bottom sediment flux q in g/m^2s at the height of the instrument is obtained as the product of the velocity module c and the SSC, in mg/L:

$$q(t) = c(t)SSC(t)$$

Averaging sediment flux over time produces the estimated magnitude of the advective flux and its direction from each sampling site during the experiment. The along-shelf and across-shelf advective sediment flux components were obtained in the same manner as the product of the SSC and the along and across components of the velocity fields. From the resulting vector (magnitude and direction) of the along and across-shelf suspended flux we can obtain the horizontal net flux for a selected interval.

Definition of sediment transport events: The sediment transport events during the study period were defined as occurring whenever the magnitude of the instantaneous sediment flux (q) at 20 m water depth exceeded 1.5 g/m^{2}s, whereas no-event intervals were defined as times when $q < 0.3$ g/m^{2}s (background level). To delimit the beginning and end of the event, a $q > 0.3$ g/m^{2}s was used. During an event, peaks of $q < 0.3$ g/m^{2}s during less than 24 h were included in the same event. In this manner, sediment transport events were extended to include both resuspension and river sediment supply events along with events of increased current activity.

Seabed erosion/deposition: The ALTUS altimeter is an autonomous 2-MHz acoustic transducer coupled with a pressure sensor. This device allows long term monitoring, but is also suitable for high-frequency surveys (sampling frequency up to 1 Hz) and has a data storage capacity of several weeks. The ALTUS provides bed elevation and water level measurements with a resolution of 0.2 and 20 mm, respectively. The transducer was positioned 22 cm above the bed, with a sampling frequency of one measurement every 15 minutes. At all sites, the pressure record for each deployment was also analysed and any evidence of tripod sinking found was removed from the seabed variation record. Thereby, any variation of the distance between the sensor and the seabed can be taken as a seabed deposition/erosion event. However, the pressure sensors at the 30 and 40 m sites were out of range during the deployments and possible tripod sinking episodes could not be identified. Thus, at 30 and 40 m depth, seabed deposition was not taken into account and seabed erosion was treated as minimum erosion.

3. Results

Physical oceanography

Masses of water of the studied zone shows the evolution from summer stratified conditions of the water column in September 2007 (Figure 2 A) to the vertical mixing in November 2007 and February 2008 (Figure 2 B and C), favoured by the cooling of surface waters and the mixing caused by storm episodes. The final situation of the study period, in spring 2008, corresponds to the onset of the water column stratification (Figure 2 D). The hydrographic structure was also modified by continental freshwater inputs from the Besòs River during the spring season, when the vertical stratification is disturbed in shallow waters (Figure 2 E).

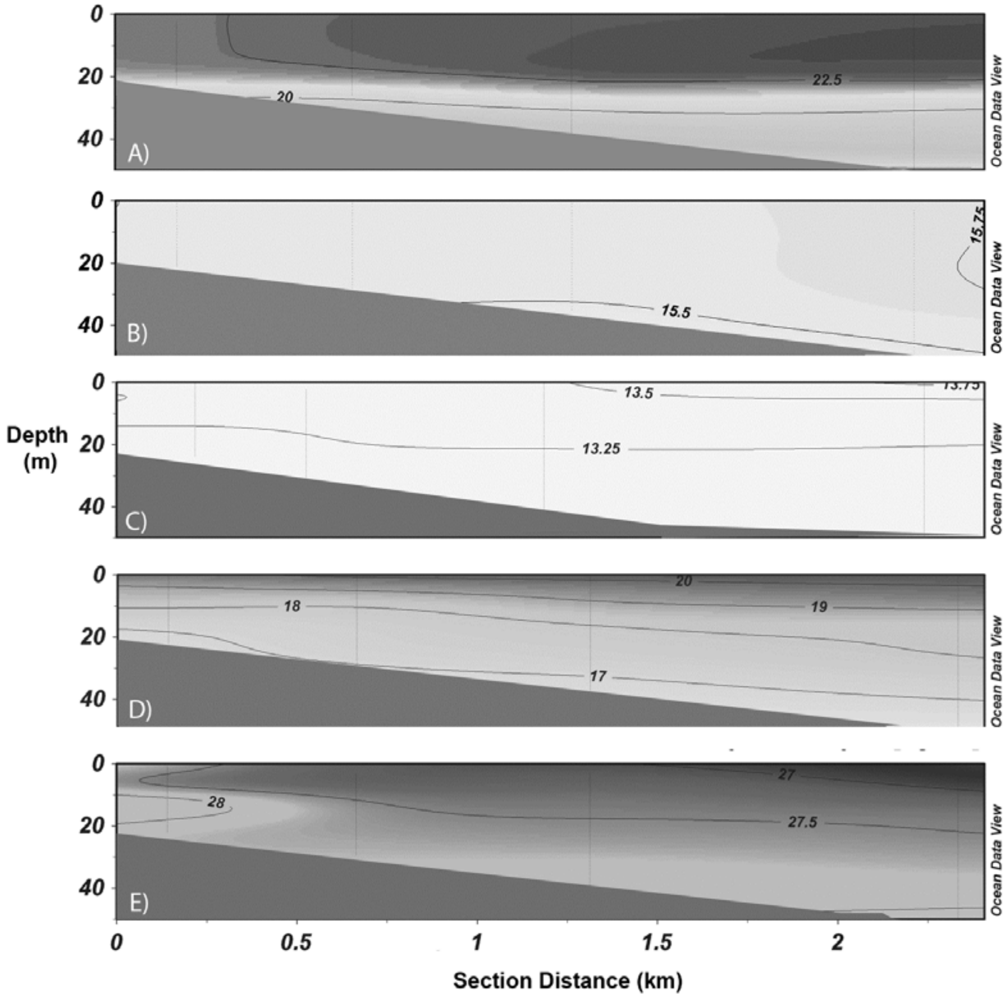

Figure 2. *Across-shelf sections of temperature (Degrees Celsius) along the tripods transect in the deployments of (A) September 2007, (B) November 2007, (C) February 2008 and (D) June 2008 and (E) potential density anomaly (kg/m3) at June 2008.*

Waves, winds and river discharge

Waves: According to wave measurements, more than 10 storm waves episodes (Hs over 2 m and Tp over 9 s) were recorded between autumn 2007 and spring 2008 (Figure 3 A and B). Of the waves propagated, 50% were from the NE-SE, 20% from the SE-S and 28% from the S-SW (Figure 4 A1). The most energetic episode occurred between 15 and 18 December 2007 and was characterized by a two-peak storm with a maximum peak of Hs of 3.38 m and a Tp of about 11 s, followed by a smaller storm (Hs > 2.5 m and Tp > 8 s) after less than 2 days of relatively calm conditions. Both storm episodes had an eastern component in the direction of wave propagation.

Winds: Wind reached speeds higher than 12 m/s during most of the storm episodes (Figure 3 C), with a blowing direction similar to the direction of wave propagation but slightly rotated (Figure 4), i.e. NE-ENE in the majority of the cases, though a few were from the SW. Although about another 20% of the wind record fell into the third quadrant (Figure 4 B2), no significant events were associated with these wind directions. In addition, diurnal winds (breezes) were relatively common in early autumn and spring but not correlated with significant wave events, as shown in the across-shelf wind component in Figure 5 A.

Besòs River discharge: The Besòs River water discharge measurements showed a typically episodic pattern, with discharge pulses occurring mainly in autumn and spring (Figure 3 D). Average river water discharge during the study period was 3.8 m^3/s, with mean daily discharge peaks of 15 and 18 m^3/s in October 2007 and May-June 2008, respectively. In October 2007, the increments in river water discharge were characterized by short, fast water pulses accompanied by increases in wave activity. River discharges lasted longer in spring 2008 than in autumn 2007, especially those of June 2008, which occurred under low-energy wave conditions.

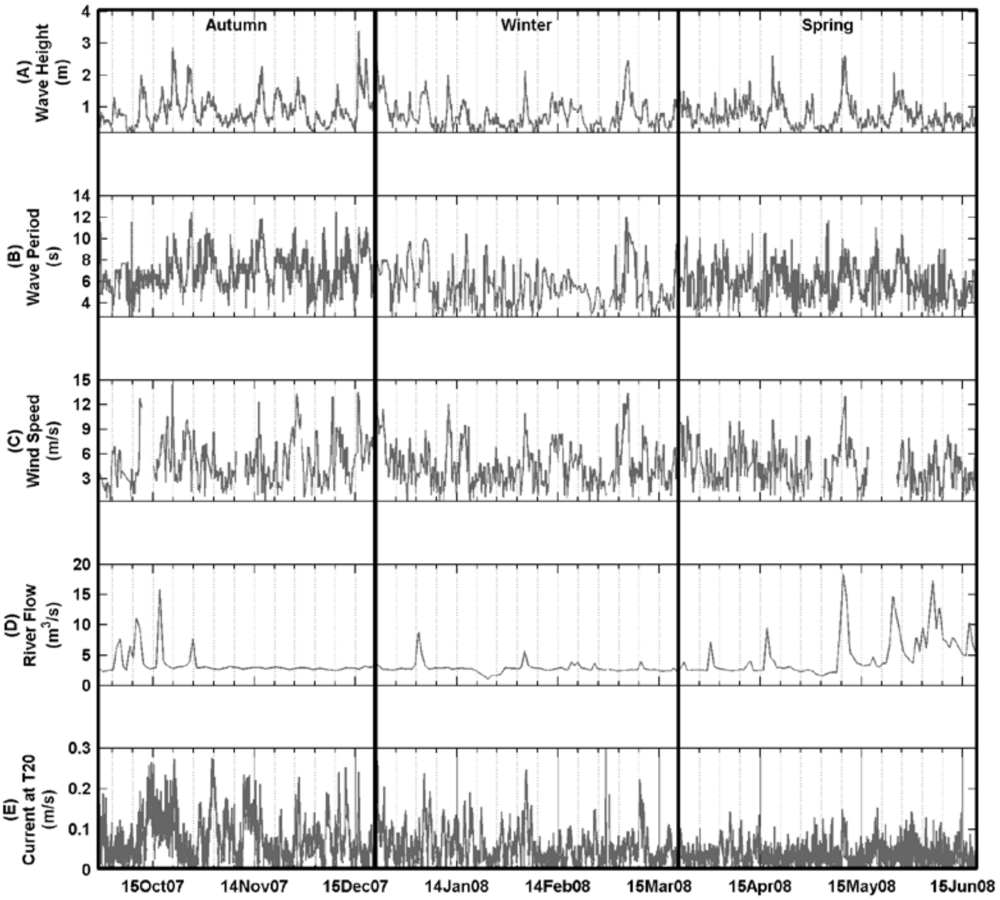

Figure 3. Meteo-oceanographic conditions during the experiment. (A) Significant wave height and (B) wave peak period at WANA point 2066051 calibrated with Llobregat buoy data; (C) wind speed at WANA point 2066051; (D) river water discharge at 2.8 km upstream from the Besòs River mouth; and (E) current speed at tripod site T20 (20 m isobath).

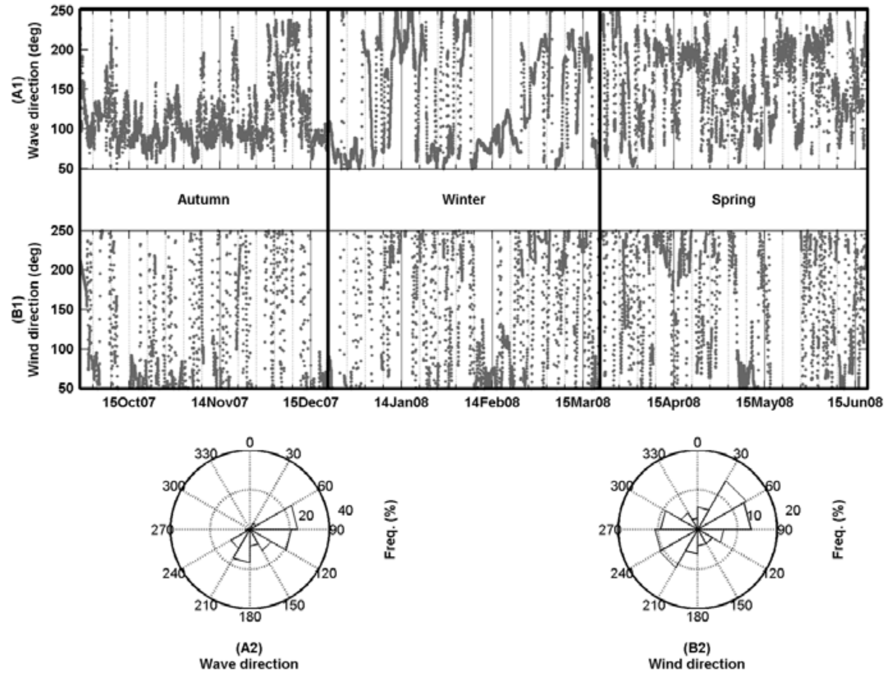

Figure 4. Time series of wave directions at WANA point 2066051 calibrated with Llobregat buoy data (A1) and wind directions (B1) at WANA point 2066051 during the study period. (A2) and (B2) rose diagram of the relative frequency of the records of wave and wind directions, respectively.

Near-bottom currents

The time series of current speed measured at 0.58 mab from the T20 site (20 m water depth) is shown in Figure 3 E. At that site, near-bottom current speed averaged 0.071 m/s with peaks associated with storm wave events on the inner shelf. At the T30 and T40 sites, current speeds showed similar values (averaged value are 0.056 m/s and 0.067 m/s in T30 and T40 respectively). In the three stations the standard deviation and the maximum current peaks are similar: 0.045 m/s in T20, 0.044 m/s T30 and 0.056 m/s in T40 for the standard deviation and peaks up to 0.279 m/s, 0.281 m/s and 0.309 m/s, respectively. In T20, the current intensity decreases in spring compared to autumn and winter observations (seasonal averaged intensity is 0.039 m/s).

Across the inner shelf, both current components were variable in time during the study period, particularly the along-shelf component (Figure 5 A). The along-shelf current speed reached more than 0.20 m/s at all sites in autumn and winter and diminished in intensity in spring. However, across-shelf velocities were under 0.10 m/s throughout the study period at T20 and up to 0.15 m/s in autumn and winter at sites T30 and T40 (Figure 5 A). Therefore, evident differences in near-bottom current velocities were found between the T20 site respect to the other sites, where the along-shelf variability was much larger than the across-shelf variability with standard deviations of 0.067 m/s and 0.025 m/s, respectively. While, in the T30 and 40 m T40 sites the across-shelf velocities were stronger and presented more variability, with standard deviations of 0.068 m/s and 0.086 m/s in the along-shelf component and 0.037 and 0.041 in the across-shelf current, respectively. The progressive current vectors shown in Figure 5 B stressed the above-mentioned temporal and spatial variability across the shelf. In autumn (from Sep07 to Dec07 annotations in Figure 5 B), offshore flows controlled the across-shelf component at 20 m water depth, while in deeper waters (sites T30 and T40), onshore flows were dominant in the across-shelf direction. At all sites, the resulting along-shelf flows were northeastward in early autumn and southwestward in late autumn. During winter (from Dec07 to Mar08 annotations in Figure 5 B), an evident reversal among the sites in current direction occurred, with the prevalent directed offshore at 20 m depth but southwestward (i.e. along-shelf) at 30 m depth. During this period, the main difference between the two sites was an increase in the along-shelf current intensity at 30 m depth in comparison with the previous period. In spring (from Mar08 to Jun08 in Figure 5 A), at the 20 m site the across-shelf current intensity increased progressively, while the along-shelf current intensity decreased during this period. In relation to the direction of the current, both along and across components showed a reversion in the flow direction, northeastward and seaward, respectively.

Although visual correspondence is observed between near-bottom along-shelf flow and the along-shelf wind direction (see wind decomposition in Figure 5 A) during some peaks of the time series, the current intensity is poorly correlated with the wind with correlation coefficients under 0.02 for both components at all three sites. The divergence between the wind and the near-bottom current observations may be originated by several factors such has the role that play the pressure gradient that may drive the flow under particular circumstances, the bathymetric effect that modify the flow direction, the role of the stratification that inhibit the momentum transfer from surface to bottom or the topographic coastal waves (see discussion in Grifoll et al., 2012; 2016).

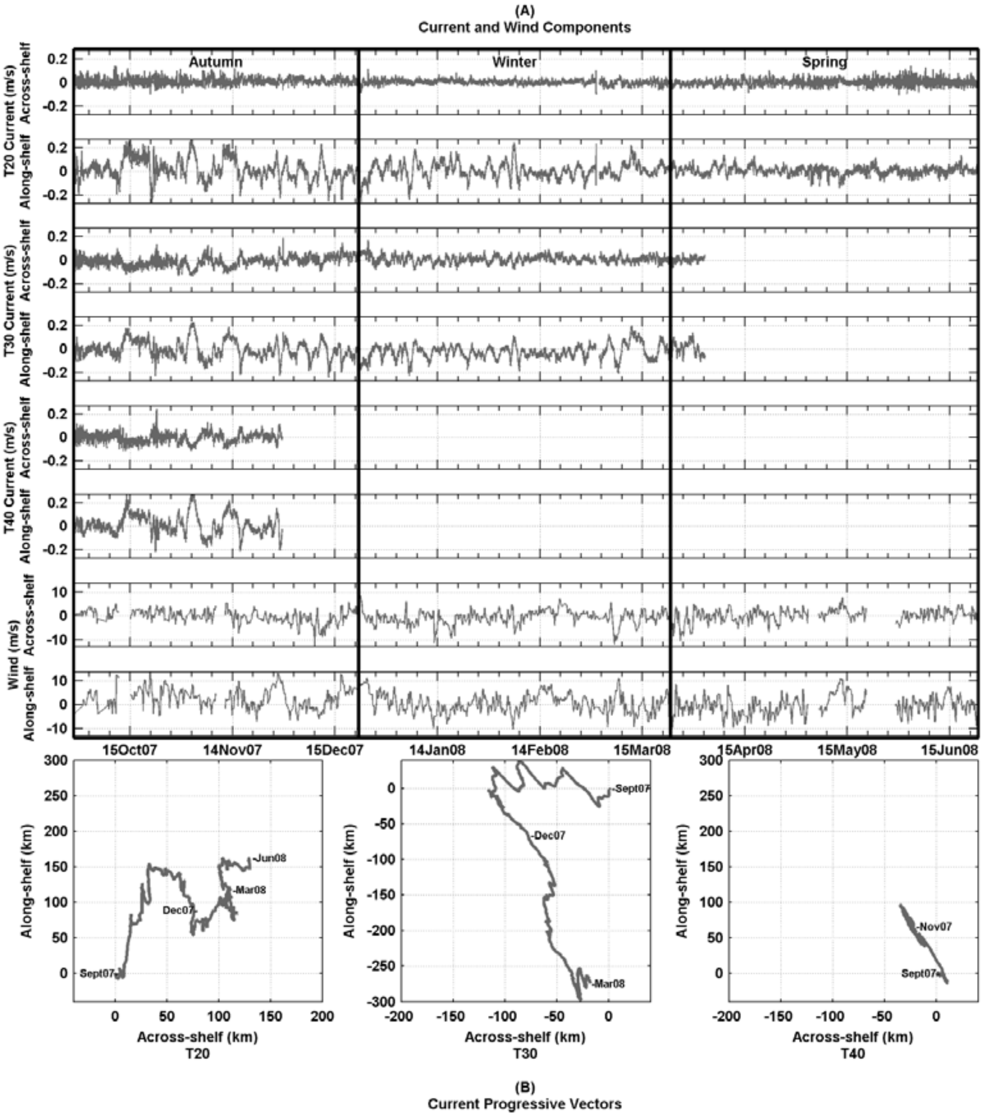

Figure 5. (A) Times series of across-shelf and along-shelf near-bottom current and wind components and (B) current progressive vectors in those directions at the T20, T30 and T40 tripod sites, respectively. Positive values are northeastward (along-shelf) and offshore.

Total maximum bottom shear stress

Estimations of the bottom shear stress reveal that wave-induced stress dominated over current-induced stress at all sites (Figure 6 at T20 site. T30 and T40 data not shown), with wave shear velocities (U_{*w}) generally 2 times larger than current shear velocities (U_{*c}) at 20 m water depth. Comparing periods with available data across the shelf (i.e. October and

November 2007), wave shear stress averaged 0.11 N/m^2, 0.06 N/m^2 and 0.04 N/m^2 and reached values of 1.02 N/m^2, 0.43 N/m^2 and 0.32 N/m^2 at 20 m, 30 m and 40 m water depths, respectively. At all sites, autumn 2007 was characterized by a high frequency and intensity of bottom shear stress. The total maximum bed shear stress was reached during the 15–18 December 2007 episode, with a maximum peak of 1.77 N/m^2 at T20 and of 0.99 N/m^2 at T30. The shear stress decreased significantly in winter and spring 2008, as shown in the time series at 20 m water depth (Figure 6).

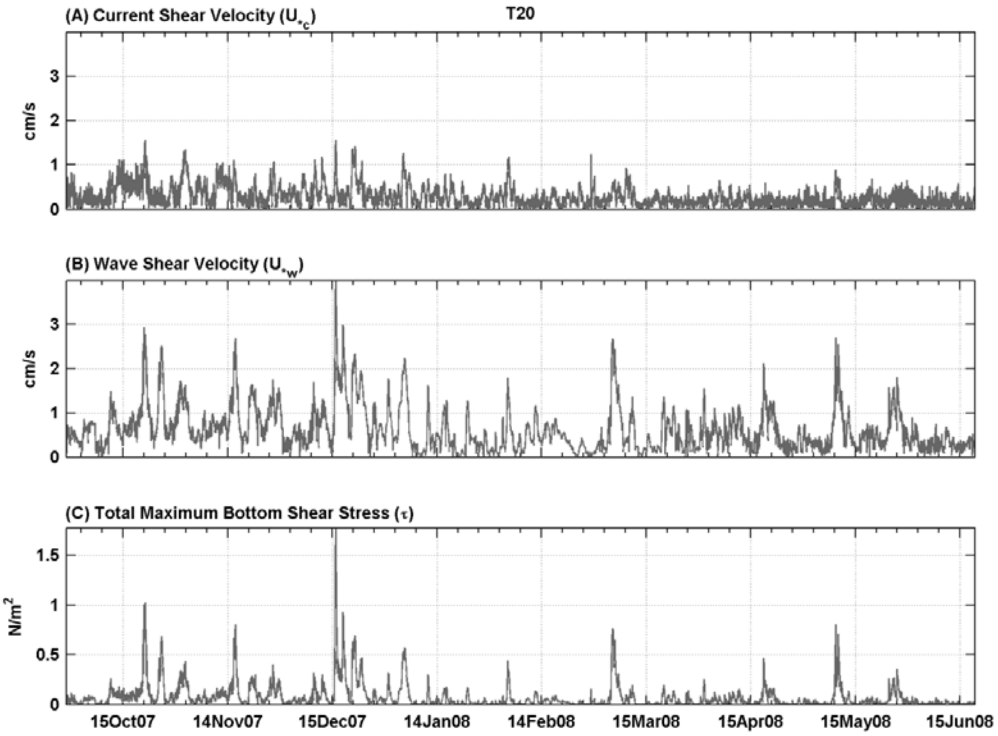

Figure 6. Time series at the T20 site (20 m water depth) of: (A) Current Shear Velocities, (B) Wave Shear Velocities and (C) Total Bottom Shear Stress.

Bottom sediment

The bottom sediment grain size displayed a general fining trend from the shallowest site towards the offshore sites, although a high spatial and temporal variability was observed during the study period (Figure 7). At the 20 m water depth site the bottom sediment became finer between September and November 2007 (with median grain sizes changing from 0.12 to 0.02 mm) and coarsening during winter, ending in a uniform layer of fine sand (0.14 mm) in spring 2008. At the 30 m site, there was a coarsening trend of the 2-3 surface centimetres from November 2007 to February 2008 (D50=0.06–0.14 mm), ending in a finer quasi-uniform median grain size distribution in the sediment column in spring 2008 (D50=0.02–0.04 mm). Finally, no major changes in grain size were observed at the deepest site (40 m depth) because the grain size variability was within a very fine sediment range (D50=0.015–0.025 mm). However, the observed trend was also a coarsening towards the end of the record (spring 2008), when the thin layers of clayey sediment detected in previous sampling surveys (<0.01 mm) disappeared (Figure 7).

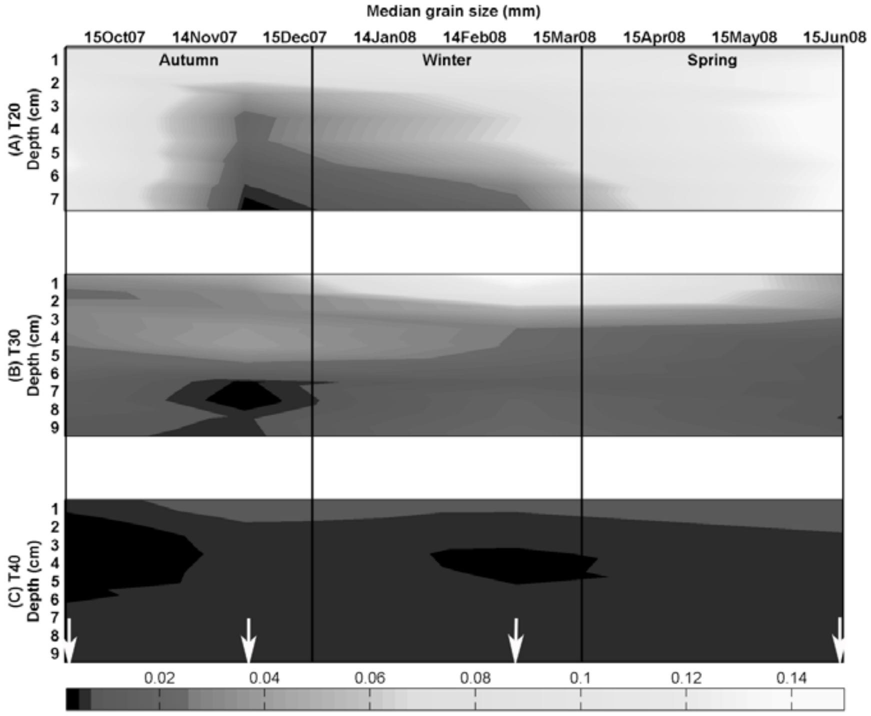

Figure 7. Temporal variability of median grain size (d50 in mm) between 0 and 10 cm depth of the cores sampled at 20, 30 and 40 m water depth. White arrows indicate the date when the samples were taken. The colorbar indicates median grain size in mm.

Near-bottom suspended sediment concentration

The near-bottom suspended sediment concentration (SSC) during the recording period showed a high temporal and spatial variability. At the 20 m water depth site, noticeable SSC was observed in autumn 2007 and spring 2008, with maximum peaks of up to 80 mg/L (25–26 October 2007) and 100 mg/L (9–10 May 2008), whereas the SSC decreased significantly in winter, with limited peaks under 40 mg/L. In general, the near-bottom SSC decreased with depth, with maximum SSC peaks below 70 and 40 mg/L at 30 and 40 m water depth, respectively. However, SSC was higher at 30 than at 20 m depth during the strongest storms. The 15–18 December 2007 episode generated a SSC of about 70 and 50 mg/L at 30 and 20 m water depth, respectively, and the 3–5 January 2008 episode generated an SSC of 40 and 20 mg/L at 30 and 20 m water depth, respectively.

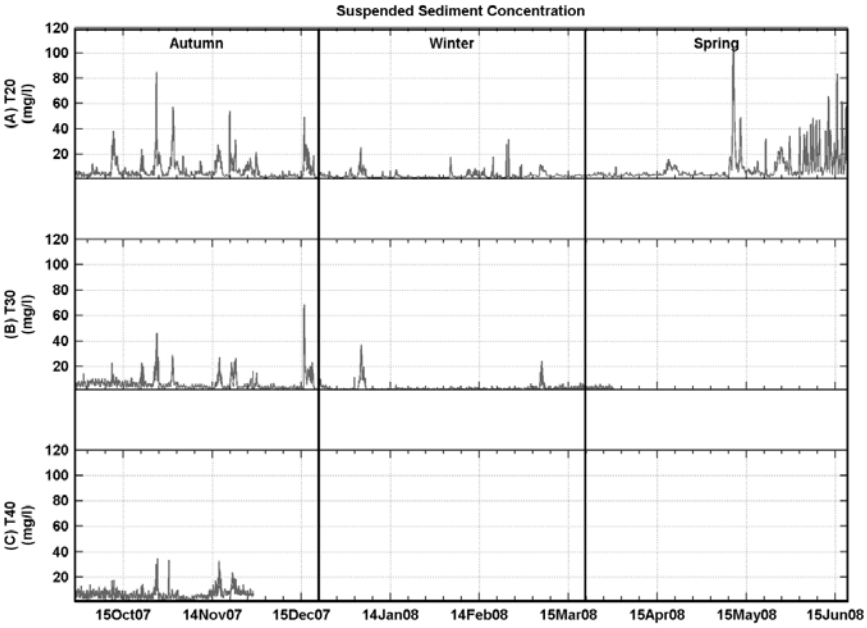

Figure 8. Time series of SSC at the three tripod sites: (A) T20 at 20 m depth, (B) T30 at 30 m depth, and (C) T40 at 40 m depth.

Seabed level

Altimeter data showed a very dynamic seabed, with significant seabed level variability across the inner shelf. Throughout the study period, the shallowest site (20 m depth) showed more dynamism in terms of frequency of erosion/deposition episodes than the 30 m site. However, the net seabed variation during the monitoring period was an erosion of about 4 and 10 cm at 20 and 30 m water depth, respectively (Figure 9 A and B). Two major seabed erosion/accumulation episodes related to the strongest storms were recorded at both sites: a) the 15–18 December 2007 episode caused a deposition of a 3 cm layer that was rapidly eroded at the 20 m site and an erosion of more than 6 cm at the 30 m site; and b) the 3–5 January 2008 episode caused an erosion of more than 2 and 3 cm at 20 and 30 m depth, respectively.

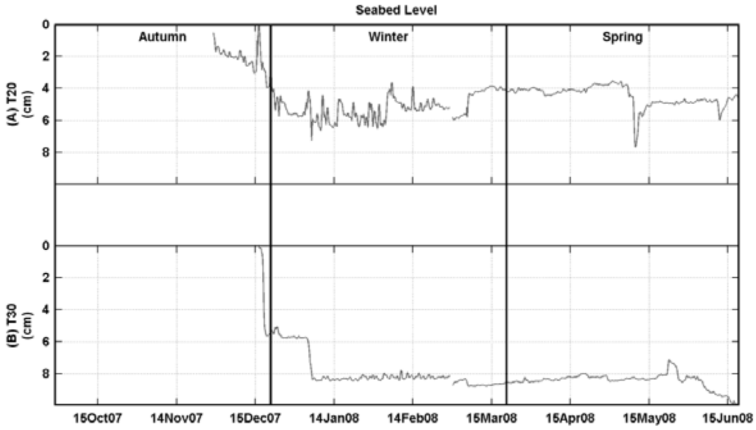

Figure 9. Seabed evolution at (A) the T20 site and (B) the T30 tripod site, at 20 and 30 m water depth, respectively.

Sediment transport events

Fourteen sediment transport events were identified (Table 2 and Figure 10, see criteria in Methods): eight in autumn 2008, two in winter 2007-2008 (January–February) and four in spring 2008 (May–June). Sediment transport events contributed 54% of the total near-bottom sediment transport and appeared to be roughly proportional to the number of events in each season. Between September 2007 and June 2008, sediment transport during events ranged from 70% in autumn, when the majority of the events occurred, to 34% in winter and 53% in spring. Similar percentages were observed for the along-shelf transport, which represented 70%, 44% and 58% of the total near-bottom transport for these seasons. Indeed, during the selected events, sediment transport intensity increased in the along-shelf component, predominantly southwestward, while during no-event intervals the offshore component prevailed (Figure 11).

Event	**Date: Start / Peak**	**Duration (h)**	**Sediment flux (g/m^2s)**	**U_{br} (m/s)**	**Wave dir**	**River water dis. (m^3/s)**	**SSC (mg/l)**	**Current (m/s)**		**Wind (m/s)**		**Type of Event**
								Speed	**Dir**	**Speed**	**Dir**	
A_1	11-Oct-07 00:18	29	*1.7*	*0.11~~6~~*	*96º*	*4.3*	*16.7*	*0.11*	*128º*	*10.0*	*43º*	Wet Storm
	11-Oct-07 21:18		**6.1**	**0.~~33~~17**	**82º**	**9.1**	**39.3**	**0.18**	**220º**	**11.1**	**46º**	
A_2	12-Oct-07 05:38	194	*0.6*	*0.~~10~~06*	*100º*	*4.7*	*5.4*	*0.13*	*49º*	*6.3*	*56º*	Wet Storm
	12-Oct-07 23:58		**2.1**	**0.~~27~~14**	**101º**	**15.8**	**10.2**	**0.26**	**43º**	**10.4**	**44º**	
B	20-Oct-07 18:38	35	*1.7*	*0.25~~48~~*	*78º*	*2.8*	*10.5*	*0.17*	*180º*	*6.3*	*69º*	Ephemeral
	21-Oct-07 07:38		**5.6**	**0.40~~72~~**	**77º**	**2.8**	**22.3**	**0.24**	**213º**	**14.4**	**59º**	
C	25-Oct-07 19:38	36	*0.9*	*0.22~~39~~*	*88º*	*4.2*	*26.3*	*0.03*	*143º*	*5.8*	*68º*	Ephemeral
	26-Oct-07 07:38		**4.4**	**0.~~60~~35**	**76º**	**7.7**	**82.3**	**0.08**	**232º**	**8.8**	**30º**	
D	31-Oct-07 12:58	72	*2.4*	*0.13~~24~~*	*100º*	*2.8*	*16.6*	*0.16*	*43º*	*4.6*	*49º*	Ephemeral
	01-Nov-07 00:58		**12.3**	**0.~~39~~22**	**132º**	**2.9**	**58.0**	**0.28**	**56º**	**8.7**	**32º**	
E	16-Nov-07 01:38	29	*2.0*	*0.26~~45~~*	*95º*	*2.9*	*19.1*	*0.10*	*202º*	*4.5*	*69º*	Ephemeral
	16-Nov-07 12:18		**4.4**	**0.37~~62~~**	**92º**	**3.0**	**27.5**	**0.21**	**217º**	**8.3**	**9º**	
F	20-Nov-07 09:58	56	*0.8*	*0.15~~30~~*	*98º*	*3.0*	*15.9*	*0.05*	*175º*	*3.0*	*217º*	Dry Storm
	22-Nov-07 10:38		**3.9**	**0.21~~40~~**	**87º**	**3.0**	**57.7**	**0.15**	**221º**	**7.5**	**202º**	
G	26-Nov-07 00:18	90	*0.7*	*0.12~~24~~*	*100º*	*2.9*	*8.5*	*0.08*	*103º*	*6.9*	*77º*	Dry Storm
	27-Nov-07 16:58		**1.8**	**0.20~~40~~**	**83º**	**3.0**	**21.6**	**0.23**	**216º**	**13.3**	**37º**	
H_1	15-dec-07 15:38	93	*1.0*	*0.26~~43~~*	*89º*	*3.0*	*13.0*	*0.06*	*167º*	*7.3*	*52º*	Dry Storm
	15-dec-07 22:58		**9.1**	**0.59~~91~~**	**87º**	**3.0**	**48.9**	**0.24**	**224º**	**13.5**	**60º**	
H_2	20-dec-07 16:38	74	*0.5*	*0.20~~34~~*	*84º*	*3.1*	*3.5*	*0.14*	*222º*	*10.3*	*58º*	Dry Storm
	21-dec-07 11:58		**1.8**	**0.28~~49~~**	**109º**	**3.1**	**7.8**	**0.27**	**217º**	**13.8**	**86º**	
I	03-jan-08 17:18	61	*0.8*	*0.19~~33~~*	*104º*	*3.7*	*8.0*	*0.10*	*187º*	*5.4*	*264º*	Dry Storm
	04-jan-08 08:18		**3.0**	**0.29~~48~~**	**55º**	**6.1**	**24.1**	**0.24**	**219º**	**8.9**	**351º**	

J	03-Feb-08 22:37	21	*1.3*	*0.13~~22~~*	*205º*	*3.8*	*6.9*	*0.19*	*49º*	*8.9*	*250º*	Dry Storm
	04-Feb-08 03:17		**4.0**	**0.19~~32~~**	**191º**	**5.7**	**17.8**	**0.25**	**51º**	**10.9**	**202º**	
K	09-May-08 12:39	48	*2.3*	*0.21~~40~~*	*129º*	*15.0*	*36.2*	*0.08*	*208º*	*8.8*	*79º*	Wet Storm
	10-May-08 23:38		**15.2**	**0.3~~6~~7**	**131º**	**18.4**	**103.7**	**0.15**	**201º**	**13.0**	**78º**	
L	25-May-08 22:19	86	*0.6*	*0.~~24~~12*	*121º*	*7.2*	*15.5*	*0.04*	*168º*	*4.1*	*227º*	Wet Storm
	27-May-08 10:18		**2.4**	**0.23~~41~~**	**111º**	**11.8**	**38.0**	**0.12**	**182º**	**7.7**	**241º**	
M	03-Jun-08 19:39	157	*0.6*	*0.02~~3~~*	*171º*	*10.6*	*17.5*	*0.03*	*158º*	*3.6*	*159º*	River Discharge
	04-Jun-08 07:59		**6.9**	**0.07~~14~~**	**150º**	**17.3**	**47.8**	**0.13**	**143º**	**7.7**	**240º**	
N	12-Jun-08 04:39	129	*0.7*	*0.01~~2~~*	159º	*6.7*	*20.5*	*0.04*	113º	*3.4*	*164º*	River Discharge
	15-Jun-08 13:59		**7.2**	**0.04~~5~~**	**212º**	**10.4**	**82.1**	**0.14**	**53º**	**7.2**	**222º**	

Table 2. Characteristics of sediment transport events at 20 m water depth from September 2007 to June 2008. Italic and bold numbers correspond to mean and maximum values, respectively. Note that events A and H were divided into two sub-events due to the occurrence of significant changes in the hydrodynamics during these events.

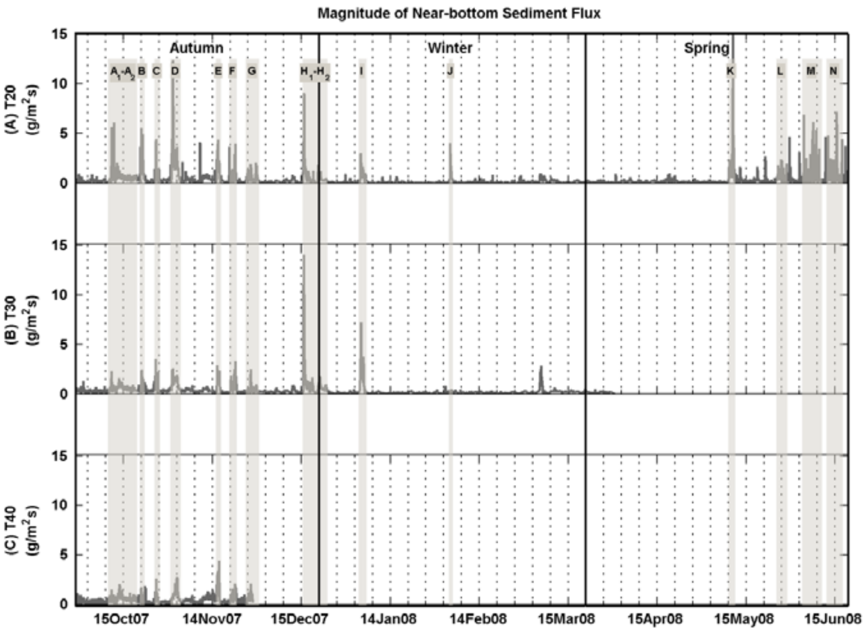

Figure 10. Time series of near-bottom sediment flux magnitude at the three tripod locations. (A) 20 m depth, (B) 30 m depth and (C) 40 m depth. Grey lines and ~~L~~letters indicate the selected sediment flux events defined at the 20 m depth site.

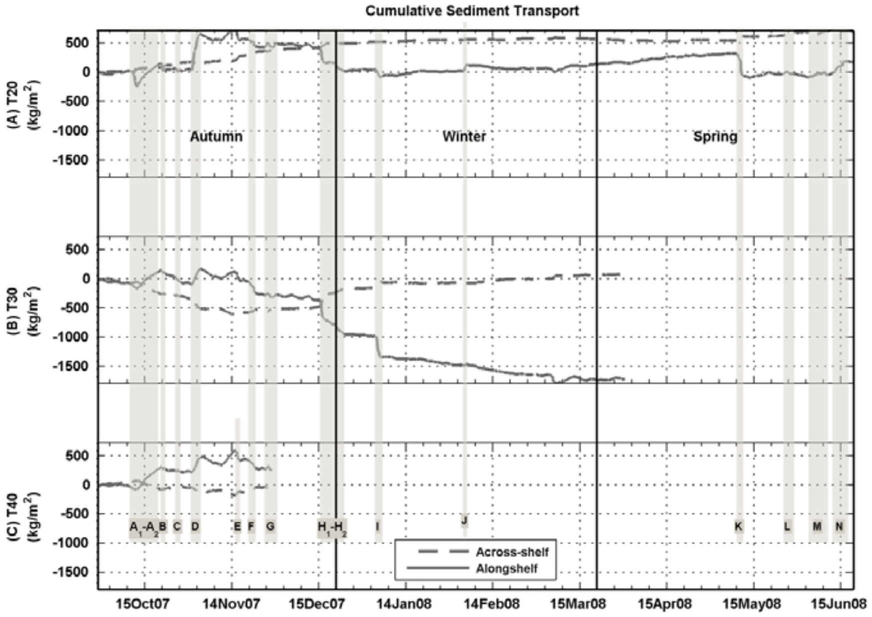

Figure 11. Along-shelf and across-shelf cumulative sediment transport near the bottom for the recording period at (A) the 20 m site, (B) the 30 m site and (C) the 40 m site. Positive values northeastward in the along-shelf direction and in the offshore direction. Grey lines and ~~L~~letters inside the plots represent the selected events.

4. Discussion

SSC and shear stress: Influence of fresh sediment availability

The magnitude of sediment fluxes depends on the across-shelf gradient in wave energy and current speed but also on the availability of suspendable sediment (Harris and Wiberg, 2002). On the Barcelona inner shelf, the magnitude of sediment fluxes was clearly influenced by the availability of river-derived fresh sediment and was associated with increases in river discharges, wave and current energy (dry storms), and the coupling of the two processes (wet storms). This is the reason for the higher SSC at 30 m than a 20 m water depth observed during some events (see section 3). The influence of sediment availability on the magnitude of sediment fluxes can be analysed qualitatively by plotting the relation between the SSC and shear stress during different types of events (Figure 12). An overall relation is derived from the plot, although several conclusions can be drawn when types of sediment flux events are considered. Four types of sediment flux events were differentiated (Table 2): A) high river discharge and low waves (river discharges), B) high river discharge and storm waves (wet storms), C) storm waves with ephemeral bottom layer (ephemeral layers) and D) storm waves (dry storms).

The SSC was high during increases in river discharges and very low shear stresses (Figure 12 – River Discharges). Under these conditions, a temporal near-bottom nepheloid layer developed where the SSC reached high values (unrelated to shear stress) that lasted as long as the increase in river discharge. Sediment fluxes during these types of event were moderate but long-lasting and accounted for 9% of the total sediment transport during the analysed events.

The maximum observed SSC was reached during periods of riverine inputs and moderate wave storms (Figure 12 – Wet Storms). This finding was interpreted as a result of the combination of resuspension processes and the maintenance of a near-bottom nepheloid layer with riverine and bottom particles. In these events, peaks of SSC and shear stress nearly matched. In many cases, an additional peak in the SSC was observed after the maximum peak of the storm (Figure 12 B) due to the advection of riverine sediment, as observed on other shelves (Ogston and Sternberg, 1999). Sediment fluxes during wet storms accounted for 38% of the total sediment transport during events. Indeed, the most noteworthy sediment transport event occurred under a wet storm that was not the most energetic event in terms of shear stress.

The availability of fresh sediment through the formation of ephemeral bottom layers also affected the magnitude of SSC and sediment fluxes during some intermediate-intensity storms during the study period. The formation of flood-derived fine deposits offshore of the Besòs River system previous to a storm passage could enhance the bottom sediment erodibility and SSC because of the higher porosity and water content of the fresh sediment (Grifoll et al., 2014; Guillén et al., 2006). During these events, the presence of ephemeral layers changed bottom sediment erodibility and SSC reached higher values than expected due to wave-current conditions (Figure 12 – Ephemeral). The influence of these ephemeral layers, and therefore of river-derived fresh sediment, was observed in both shallow and deeper inner shelf waters. Once the fresh sediment was eroded and transported offshore, the available fresh sediment, now in deeper areas, increased the SSC in comparison with shallow waters, changing the across-shelf gradient of sediment fluxes (higher sediment flux in deeper water during events H and I – Figure 10). Sediment fluxes during events influenced by ephemeral layers accounted for 29% of the total transport during events.

Finally, the maximum shear stress occurred during dry storms events, in which SSC and shear stress peaks coincided (Figure 12 D), suggesting that resuspension of bottom sediment controls SSC. The near-bottom sediment flux during dry storms accounted for 24% of the total sediment transport during events.

Actually, the proportionality between SSC and shear stress is observed when individual wave storms events are considered. However, this proportionality disappears when all events are taken into account, mainly because of changes in conditions of fresh sediment availability. The influence of fresh sediment availability in sediment dynamics can be evaluated in terms of the percentage of suspended sediment fluxes with or without available fresh sediment (river discharges or ephemeral layers), which accounted for 76% of the sediment transport events. In fact, only 5 of the 14 defined sediment transport events occurred without a direct influence of riverine inputs.

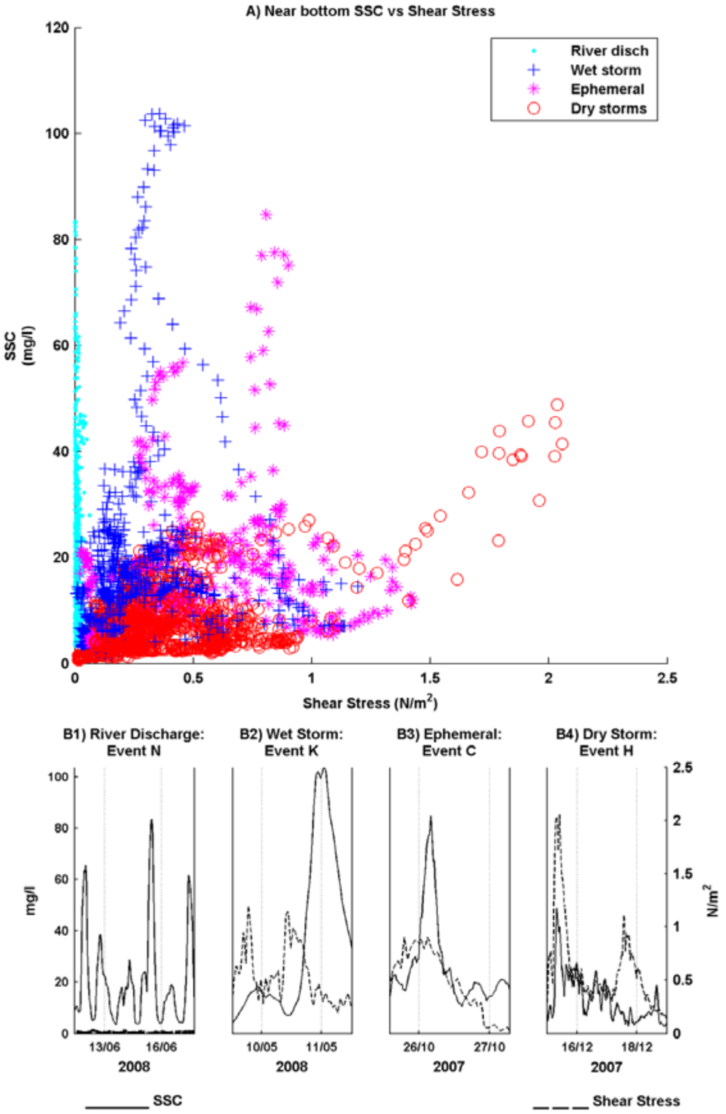

Figure 12. A) The relation between suspended sediment concentration (SSC) and bottom shear stress according to the four types of sediment transport events identified on the Barcelona inner shelf: high river discharge and low waves, wet storms, storms with ephemeral bottom layers, and dry storms. B1, B2, B3 and B4) Time series of SSC, shear stress and river discharge for one of each type of sediment transport events.

Seasonality of sediment dynamics

The resulting near-bottom sediment transport on the Barcelona inner shelf off the Besòs River was mainly directed southwestward (along-shelf) during the study period. This fact is consistent with previous observations on low-energy shelves, where along-shelf sediment flux is stronger than across-shelf flux, in contrast to high-energy shelves (Allison et al., 2000;

Fain et al., 2007; Ogston and Sternberg, 1999; Ogston et al., 2000; Palanques et al., 2002; Sherwood et al., 1994; Traykovski, et al., 2000;). The seaward component of sediment flux on the Besòs shelf was indeed low but favoured the segregation of coarse and fine sediment from the nearshore towards deeper waters, as observed in the temporal variability of the sediment grain size across the inner shelf (Figure 7). In fact, previous studies carried out in the area described a mud belt between 30 and 60 m water depth that was shifted southwestward by the dominant along-shelf transport (Checa et al., 1988; Liquete et al., 2007; Grifoll et al., 2014; Palanques and Díaz, 1994).

However, the sediment dynamics of “small” Mediterranean river systems such as the one studied show a seasonal variability (Guillén et al., 2006). In the Besòs River system, the temporal variation of the hydrographic structure, the magnitude of the forcing conditions, the observed SSC and fluxes, and the seabed evolution indicate strong seasonal variability in sediment dynamics controlled by the type, frequency and intensity of sediment transport events. Wet storms events occurred basically in autumn and spring while in winter, dry storms were the main forcing mechanism for sediment transport. Consequently, the averaged near-bottom sediment fluxes were higher in autumn and spring than in winter during the study period (Table 3). The seasonal variability is also evident in the distribution of the across-shelf magnitude of sediment fluxes, which decrease and increase between 20 and 30 m water depth in autumn and winter, respectively.

NEAR-BOTTOM FLUXES	**TYPE OF EVENTS**							**SEASONS**				
	Wet storm	**Ephemeral**			**Dry storm**		**River Disch.**	**Autumn**		**Winter**		**Spring**
	20 m	**20 m**	**30 m**	**40 m**	**20 m**	**30 m**	**20 m**	**20 m**	**30 m**	**20 m**	**30 m**	**20 m**
Mean along-shelf flux	1.63	1.79	0.94	0.84	0.69	0.91	0.40	0.47	0.38	0.14	0.19	0.22
Mean across-shelf flux	0.88	0.39	0.49	0.34	0.15	0.43	0.37	0.14	0.22	0.04	0.08	0.16
Averaged flux	2.07	1.90	1.09	0.92	0.74	1.03	0.60	0.52	0.46	0.15	0.22	0.29
Net flux	320	268	109	45	379	795	200	425	694	61	822	114
Net direction	125	112	47	135	149	159	136	60	208	47	153	66

Table 3. Near-bottom sediment fluxes: Mean and averaged sediment flux ~~in~~ (g/m^2s) and net flux magnitude (g/m^2 for the especific time interval) and direction (degrees) with respect to north at the tripod locations.~~, for each type of event and by season.~~

This temporal and spatial distribution of sediment fluxes on the Barcelona inner shelf is analysed as follows through the description of sediment dynamics in autumn, winter, spring and summer.

Autumn

The pattern of sediment dynamics in autumn 2007 was characterized by early riverine inputs that formed ephemeral sediment layers on the inner shelf, with subsequent resuspension and partial offshore transport at 20 m water depth, which mainly switched southwestward between 30 and 40 m water depth until resuspendable sediment was depleted. The along-shelf transport was twice as high as the across-shelf transport but the predominant offshore component in late autumn favoured the dispersion of riverine sediments towards deeper water. At the beginning of this season, the strong stratification in the water column and the combined action of moderate waves and currents resulted in a convergence of the sediment flux between 20 and 30 m water depth. Thus, the spread of the riverine sediment was prevented, probably leaving a deposit of fresh sediment in shallow waters that allowed the instantaneous sediment flux to reach values of about 12 g/m^2s at the shallowest site (20 m depth), while at 30 and 40 m water depths it was under 5 g/m^2s (event D – Figure 10). In the subsequent storm events sediment fluxes were lower than expected considering bottom shear stress probably because the ephemeral sedimentary layer was already eroded..

Winter

Winter conditions in 2008 were characterized by a homogeneous water column, low river water discharges and moderate wave activity. Two wave storm episodes with prevailing northeasterly winds that favoured stronger along-shelf over across-shelf flow (events I and J) lasted 2 days and 1 day, respectively. The pattern of sediment transport was similar to that in late autumn 2007, with limited fine-grained sediment in shallow waters and sediment transport predominantly towards the southwest. The variability in the intensity of sediment fluxes across the shelf is consistent with the seabed changes observed during this season, (Figure 7 and 9). The across-shelf bottom sediment distribution caused the excess of shear stress to increase offshore during this event and, consequently, sediment fluxes were higher at 30 than at 20 m water depth (7 g/m^2s and 3 g/m^2s, respectively), with a prevalent near-bottom southwestward current at both sites.

Spring

Spring 2008 was characterized by the onset of the stratified conditions of the water column, moderate winds and waves, and prolonged high river water discharge. The river discharge and wind regime were typical of those occurring during the Mediterranean spring season (Cerralbo et al., 2015; Font, 1990; Liquete et al., 2009;), with a predominant southeasterly wind direction during low-pressure system passages and sea breezes in the diurnal bands. However, the spring 2008 events were characterized by moderate wind energy in both frequency bands. Seabed variations and sediment flux measurements from May to June 2008 suggest a multi-step deposition-erosion-transport pattern across the inner shelf. The mechanisms responsible for the high sediment transport at 20 m water depth (in relation to moderate shear stress) may be related to the high river flow (up to 5 m^3/s) between May and June 2008, which could have contributed to the maintenance of high SSC in the water column and the formation of an ephemeral sediment layer progressively migrating offshore. In June 2008, the thermocline was around 30 m depth and was associated with high near-bottom SSC (Figure 2 D). It could therefore be hypothesized, as suggested in previous studies (Puig et al., 2001; 2007; Urgelés et al., 2011), that processes linked to the thermocline such as internal waves favour bottom sediment remobilization and the maintenance of a bottom nepheloid layer.

Summer

Although no full observations were obtained in summer 2008, the Mediterranean climate is characterized by dry summers with well-developed sea breezes (Cerralbo et al., 2015; Font, 1990) and relatively stable atmospheric conditions. In summer 2008, measured wave conditions below a significant wave height of 1.3 m and mean river water discharge (2.31 m^3/s) were consistent with the summer season in the area (Bolaños et al., 2008; Sánchez-Arcilla et al., 2008). Thermal stratification developed on the shelf due to the increase in heat fluxes, as occurred seasonally (Grifoll et al, 2014; Salat et al. 2002). In consequence, under these conditions we can infer that significant sediment transport events were not expected during the summer period.

5. Conclusions

This study shows the complexity of “small” Mediterranean river systems in the sediment dispersal from the continent to the sea. This complexity gives rise to a set of sediment resuspension and transport mechanisms with a strong seasonal variability. In early autumn, evidence of the formation of temporal nepheloid layers and ephemeral sediment bottom layers was found, indicating increased availability of fine sediment near the bottom to interact with resuspension and transport processes. In late autumn and winter events, high bed shear stresses and prevalent southwestern and offshore currents resuspended and winnowed the ephemeral layers previously deposited in shallow waters. In spring, large river discharge episodes were more frequent, and most of them occurred under low-energy wave conditions. In these cases additional processes such as diurnal winds and/or hydrographic conditions may have controlled sediment transport. This seasonal variability leads to a temporal evolution of the bottom grain size (coarser during winter) and the near-bottom sediment transport rates (higher in autumn and spring), which are consistent with the hydrodynamic seasonal events and the river discharge regime.

In the Besòs River system, more than 50% of the total near-bottom suspended sediment transport from September 2007 to July 2008 occurred in 14 storm events, which represented the 54 % of the total sediment transport along the study period. The contribution of the events, however, differed along each season, which represented the 70 %, 34 % and 53 % in autumn, winter and spring, respectively. Of these events, about 75% were directly influenced by riverine inputs through temporal nepheloid layers and/or ephemeral bottom layers, highlighting the importance of the availability of fresh riverine sediment in near-bottom suspended sediment transport rates across the inner shelf. In general, sediment transport and seabed changes were lower when riverine fresh sediment was not available across the inner shelf. Nonetheless, when riverine sediment was available in the nearshore, sediment transport rates were enhanced in shallow waters (20 m water depth) and the across-shelf sediment transport rate decreased offshore. In contrast, when fresh sediment had been winnowed from shallow areas (20 m water depth) and deposited offshore (30 m water depth), sediment transport and seabed erosion were higher offshore as the sediment availability increased there.

These results show that small rivers delivering sediment into the Mediterranean basin enhance near-bottom suspended sediment transport rates by increasing the SSC and decreasing threshold conditions for bottom sediment resuspension. In the Mediterranean almost tideless area with weak currents, river discharge and wave climate control the availability of sediment to be resuspended and transported to other parts of the inner-shelf. Both of these controlling factors are seasonal, so sediment dynamics on the inner shelf also displays seasonality.

Acknowledgements

This work was supported by the *Ministerio de Educación y Ciencia* of the Spanish Government within the SEDMET project (CTM2006-06919). The authors would like to thank Óscar Ferreira (CIMA-UALG, Portugal) and Henko de Stigter (NIOZ, the Netherlands) for their comments and suggestions on an initial draft. The manuscript was also improved by suggestions from all members of the committee for the defence of the doctoral thesis in which this paper was presented among other results. The research leading to these results obtained data from the *Xarxa d'Instruments Oceanogràfics i Meteorològics* (*Generalitat de Catalunya*), which is currently out of service. We also thank the officers and crew of the R/V *García del Cid* (CSIC) and the R/V *Sarmiento de Gamboa* (MINECO) and the staff of the *Institut de Ciències del Mar* (CSIC) and the *Unitat de Tecnologia Marina* (CSIC) for their help and dedication during the cruises and in the laboratory work. L.L, A.P. and J.G belong to CRG on Littoral and Oceanic Processes, supported by Grant 2014 SGR 1642 of the *Generalitat de Catalunya*.

References

Allison, M.A., Kineke, G.C., Gordon, E.S. and Goñi, M.A. (2000). Development and reworking of a seasonal flood deposit on the inner continental shelf off the Atchafalaya River. Continental Shelf Research 20, 2267–2294.

Antonijuan, J., Guillén, J., López, L. and Simarro, G. (2012). Near-bottom sediment dynamics on highly-protected beaches The Coastal Ocean Observatory of Barcelona. IEEE Instrumentation and Measurement Technology Conference 2012, 403 – 406.

Bever, A.J., McNinch, J.E. and Harris, C.K. (2011). Hydrodynamics and sediment-transport in the nearshore of Poverty Bay, New Zealand: Observations of nearshore sediment segregation and oceanic storms. Continental Shelf Research 31, 507–526.

Bolaños, R., Jorda, G., Cateura, J., Lopez, J., Puigdefabregas, J., Gomez, J. and Espino, M. (2008) The XIOM: 20 years of a regional coastal observatory in the Spanish Catalan coast. Journal of Marine Systems 77, 237–260.

Bolaños, R., Wolf, J., Brown, J., Osuna, P., Monbaliu, J., and Sanchez-Arcilla, A., (2009). Comparison of wave-current interaction formulation using the POLCOMS-WAM wavecurrent model, Coastal Engineering, World Scientific Publishing, 521–533.

Bourrin, F., Friend, P.L., Amos, C.L., Manca, E., Ulses, C., Palanques, A., Durrieu de Madron, X. and Thompson, C.E.L. (2008). Sediment dispersal from a typical Mediterranean flood: The Têt River, Gulf of Lions. Continental Shelf Research 28, 1895–1910.

Cacchione, D.A., Drake, D.E., Kayen, R.W., Sternberg, R.W., Kineke, G.C. and Tate, G.B. (1995). Measurements in the bottom boundary layer on the Amazon subaqueous delta. Marine Geology 125, 235–257.

Catalan Water Agency. Agència Catalana de l'Aigua (Generalitat de Catalunya). Consulta de dades de l'aigua i el medi (CDAM). Estació d'aforament de Santa Coloma de Gramenet (riu) (EA047). http://aca-web.gencat.cat/sdim/visor.do Last accessed: March 2016.

Cerralbo, P., Grifoll, M., Moré, J., Bravo, M., Sairouní Afif, A. and Espino, M. (2015). Wind variability in a coastal area (Alfacs Bay, Ebro River delta). Advances in Science and Research 12, 11–21.

Checa, A., Díaz, J.I., Farrán, M., Maldonado, A., (1988). Sistemas deltaicos holocenos de los ríos Llobregat, Besòs y Foix: modelos evolutivos transgresivos. Acta Geològica Hispànica. 23, 241–255.

Dufois, F., Verney, R., LeHIr, P., Dumas, F. and Charmasson, S. (2014) Impact of winter storms on sediment erosion in the Rhone River prodelta and fate of sediment in the Gulf of Lions (North Western Mediterranean Sea). Continental Shelf Research 72 , 57–72.

Fain, A.M.V, Ogston, A.S. and Sternberg, R.W. (2007). Sediment transport event analysis on the western Adriatic continental shelf. Continental Shelf Research 27, 431 – 451.

Ferré, B., Guizien, K., Durrieu de Madron, X., Palanques, A., Guillén, J., Grémare, A. (2005). Fine-grained sediment dynamics during a strong storm event in the inner-shelf of the Gulf of Lion (NW Mediterranean). Continental Shelf Research 25, 2410–2427.

Flexas, M.M., Durrieu de Madron, X., García, M.A., Canals, M. and Arnau, P. (2002). Flow variability in the Gulf of Lions during the MATER HFF experiment (March–May 1997). Journal of Marine Systems 33–34, 197–214.

Font, J. (1990). A comparison of seasonal winds with currents on the continental slope of the Catalan Sea (northwestern Mediterranean). Journal of Geophysical Research 95 (C2), 1537–1545.

Geyer, W.R., Hill, P., Milligan, T., Traykovski, P. (2000). The structure of the Eel River plume during floods. Continental Shelf Research 20, 2067–2093.

Giró, S. and Maldonado, A. (1985). Análisis granulométrico por métodos automáticos: tubo de sedimentación y Sedigraph. Acta Geològica Hispànica 20, 95-102.

Grifoll, M., Aretxabaleta, A. L., Espino, M. and Warner, J. C. (2012). Along-shelf current variability on the Catalan inner-shelf (NW Mediterranean). Journal Geophysical Research: *Oceans (1978–2012)* 117 (C9).

Grifoll, M., Gracia, V., Fernandez, J. and Espino, M. (2013_1). Suspended sediment observations in the Barcelona inner-shelf during storms. Journal Coastal Research, Special Issue 65, 1533-1538.

Grifoll, M., Aretxabaleta, A. L., Pelegrí, J.L., Espino, M., Warner, J. C. and Sánchez-Arcilla, A. (2013_2). Seasonal circulation over the Catalan inner-shelf (northwest Mediterranean Sea). Journal Geophysical Research: Oceans 118, 10, 5844-5857.

Formatat: espanyol (Espanya - alfab. tradicional)

Formatat: espanyol (Espanya - alfab. tradicional)

Formatat: anglès (EUA)

Formatat: anglès (EUA)

Formatat: anglès (EUA)

Grifoll, M., Gracia, V., Aretxabaleta, A., Guillén, J., Espino, M. and Warner, J.C. (2014). Formation of fine sediment deposit from a flash flood river in the Mediterranean Sea. Journal Geophysical Research: Oceans 119, 5837-5853.

Gómez J., Espino, M., Puigdefabregas, J., Jerez, F. (2005). Xarxa d'Instrumentació Oceanogràfica i Meteorologica de la Generalitat de Catalunya (XIOM). Boies d'onatge dades obtingudes l'any 2004. Informe Técnico.

Guillén, J., Palanques, A., Durrieu de Madron, X., Nyffeler, F. (2000). Field calibration of optical sensors for measuring suspended sediment concentration in the western Mediterranean. Scientia Marina 64 (4), 427-435.

Guillén, J., Jiménez, J.A., Palanques, A., Gràcia, V., Puig, P., Sánchez-Arcilla, A. (2002). Sediment resuspension across a microtidal, low-energy inner-shelf. Continental Shelf Research 22, 305-325.

Guillén, J., Bourrin, F., Palanques A., Durrieu de Madron X., Puig P. and Buscail R. (2006). Sediment dynamics during wet and dry storm events on the Têt inner-shelf (SW Gulf of Lions). Marine Geology 234 (1–4), 129–142.

Harris, C.K. and Wiberg, P.L. (1997). Approaches to quantifying long-term continental shelf sediment transport with an example from the Northern California STRESS mid-shelf site. Continental Shelf Research 17 (11), 1387-1418.

Harris, C.K. and Wiberg, P.L. (2002). Across-shelf sediment transport: Interactions between suspended sediment and bed sediment. Journal of Geophysical Research 107 (C1).

ITGE (1989). Mapa geológico de la plataforma continental española y zonas adyacentes, 1 :200000. Hoja 35/ 42A, Barcelona. Instituto Tecnológico GeoMinero de España, Madrid, mem. Expl, pp. 117.

Jiménez, J.A., Guillén, J., Gracia, V., Palanques, A., García, M.A., Sánchez-Arcilla, A., Puig, P., Puigdefábregas, J. and Rodríguez, G. (1999). Water and sediment fluxes on the Ebro Delta shoreface: on the role of low frequency currents. Marine Geology 157, 219-239.

Liquete, C., Canals, M., Lastres, G., Amblas, D., Urgelés, R., De Mol, B., De Batis, M., Hughes-Clarke, J.E. (2007). Long-term development and current status of the Barcelona continental shelf: a source-to-sink approach. Continental Shelf Research 27, 1779-1800.

Liquete, C., Canals, M., Ludwig, W., Arnau, P., (2009). Sediment discharge of the rivers of Catalonia, NE Spain, and the influence of human impacts. Journal of Hydrology 366, 76-88.

Liquete, C., Lucchi, R.G., Garcia-Orellana, J., Canals., M., Masque, P., Pascual, C. and Lavoie, C. (2010). Modern sedimentation patterns and human impacts on the Barcelona continental shelf (NE Spain). Geologica Acta 8 (2), 169-187.

Liste, M., Grifoll, M., and Monbaliu, J. (2014). River plume dispersion in response to flash flood events. Application to the Catalan shelf. *Continental Shelf Research* 87, 96-108.

Ogston, A.S. and Sternberg, R.W., (1999). Sediment transport events on the northern California continental shelf. Marine Geology 154, 69-82.

Ogston, A.S., Cacchione, D.A., Sterberg, R.W., Kineke, G.C. (2000). Observations of storm and river flood-driven sediment transport of the northern Californian continental shelf. Continental Shelf Research 20, 2141-2162.

Palanques, A., Plana, F., and Maldonado, A. (1990). Recent influence of man on Ebro margin sedimentation system (Northwestern Mediterranean sea). Marine Geology 95, 247-63.

Palanques, A. (1994). Distribution and heavy metal pollution of the suspended particulate matter on the continental shelf (North-Western Mediterranean). Environmental Pollution 85, 205-215.

Palanques, A. and Diaz, J.I. (1994). Anthropogenic heavy metal pollution in the sediment of the Barcelona continental shelf (Northwestern Mediterranean). Marine Environmental research 38, 17-31.

Palanques, A., Puig, P., Guillén, J., Jiménez, J., Gràcia, V., Sánchez Arcilla, A., Madsen, O. (2002). Near-bottom suspended sediment fluxes on a river-influenced, tideless fetch-limited shelf (the Ebro continental shelf, NW Mediterranean). Continental Shelf research 22 (2), 285-303.

Palanques, A., Guillén, J., Puig, P., and Durrieu de Madron, X. (2008). Storm-driven shelf-to-canyon suspended sediment transport at the southwestern end of the Gulf of Lions, Continental Shelf Research 28, 1947–1956.

Palanques, A., Puig, P., Guillén, J., Durrieu de Madron, X., Latasa, M., Scharek, R. and Martin, J. (2011). Effects of storm events on the shelf-to-basin sediment transport in the southwestern end of the Gulf of Lions (Northwestern Mediterranean). Nat. Hazards Earth Syst. Sci. 11, 843–850.

Pallares, E., Sánchez-Arcilla, A. and Espino, M. (2014) Wave energy balance in wave models (SWAN) for semi-enclosed domains – Application to the Catalan coast. Continental Shelf Research 87, 41-53.

Formatat: anglès (EUA)

Formatat: anglès (EUA)

Puig, P. and Palanques, A. (1998). Nepheloid structure and hydrographic control in the Barcelona continental margin. Marine Geology 149, 39–54.

Puig, P., Palanques, A., Sánchez-Cabeza, J.A., Masqué, P. (1999). Heavy metals in particulate matter and sediments in the southern Barcelona sedimentation system (Northwestern Mediterranean). Marine Chemistry 63, 311-329.

Formatat: anglès (EUA)

Puig, P., Palanques, A., Guillén, J. (2001). Near-bottom suspended sediment variability caused by storms and near-inertial internal waves on the Ebro mid continental shelf (NW Mediterranean). Marine Geology 178, 81-93.

Puig, P., Ogston, A.S., Guillen, J., Fain, A.M.V. and Palanques, A. (2007). Sediment transport processes from the topset to the foreset of a crenulated clinoform (Adriatic Sea). Continental Shelf Research 27, 452–474.

Roussiez, V., Aloisi, J.C., Monaco, A. Ludwig, W. (2005). Early Buddy deposits along the Gulf of Lions shoreline: a key for better understanding of land-to-sea transfer of sediments and associated pollutant fluxes. Marine Geology 222-223, 345-358.

Formatat: anglès (EUA)

Rubio, A., Arnau, P.A., Espino, M., Flexas, M., Jordà, G., Salat, J., Puigdefàbregas, J. and Arcilla, A.S. (2005). A field study of the behaviour of an anticyclonic eddy on the Catalan continental shelf (NW Mediterranean), Progress in Oceanography 66, 142–156.

Salat, J., Garcia, M. A., Cruzado, A., Palanques, A., Arın, L., Gomis, D., Guillen, J., de Leon, A., Puigdefabregas, J., Sospedra, J. and Velasquez, Z.R. (2002). Seasonal changes mass structure and shelf slope at the Ebre Shelf (NW Mediterranean), Continental Shelf Research 22, 327–348.

Sánchez-Arcilla, A., González-Marco, D. and Bolaños, R. (2008) A review of wave climate and prediction along the Spanish Mediterranean coast. Natural Hazards Earth 8, 1217–1228.

Sancho-García, A., Guillén, J. and Ojeda, E. (2013). Storm-induced readjustment of an embayed beach after modification by protection works. Geo-marine Letters 33, 159-172.

Formatat: anglès (EUA)

Sherwood, C.R., Butman, B., Cacchione, D.A., Drake, D.E., Gross, T.F., Sternberg, R.W., Wiberg, P.L. and Williams III, A.J. (1994). Sediment transport events of the northern California continental shelf during the 1990–1991 STRESS experiments. Continental Shelf Research 14, 1063–1099.

Simarro, G., Guillén, J., Puig, P., Ribó, M., Lo Iacono, C., Palanques, A., Muñoz, A., Durán, R. and Acosta, J. (2015). Sediment dynamics over sand ridges on a tideless mid-outer continental shelf. Marine Geology 361, 25–40.

Soulsby, R.L. (1997). Dynamics of marine sands. Thomas Telford Ltd., London, 249pp.

Soulsby, R.L. (2006). Simplified calculations of wave orbital velocities. TR-155. HR Wallingford Ltd., Wallingford, 12pp.

Formatat: anglès (EUA)

Spanish Port Authority. Puertos del Estado. Oceanografía y Meteorología. Banco de datos. Punto WANA 2066051. http://www.puertos.es/es-es/oceanografia/Portus/Paginas/Portus.aspx. Last accessed: March 2016.

Traykovski, P., Geyer, W.R., Irish, J.D., and Lynch, J.F. (2000). The role of wave-induced density-driven fluid mud flows for cross-shelf transport on the Eel River continental shelf. Continental Shelf Research 20, 2113–2140.

Ulses, C., Estournel, C., Durrieu de Madron, X., and Palanques, A. (2008). Suspended sediment transport in the Gulf of Lion (NW Mediterranean): impact of extreme storms and floods, Continental Shelf Research 28, 2048–2070.

Urgelés, R., Cattaneo, A., Puig, P., Liquete, C., De Mol, B., Amblàs, D., Sultan, N., and Trincardi, F. (2011). A review of undulated sediment features on Mediterranean prodeltas: distinguishing sediment transport structures from sediment deformation. Mar Geophys Res 32, 49–69.

Wiberg, P. and Smith, J.D. (1983). A comparison of field data and theoretical models for wave–current interactions at the bed on the continental shelf. Continental Shelf Research 2, 147–162.

Wiberg, P.L., Drake, D.E. and Cacchione, D.A. (1994). Sediment resuspension and bed armoring during high bottom stress events on the northern California continental shelf: measurements and predictions. Continental Shelf Research 14, 1191–1219.

Wiberg, P.L. and Sherwood, C.R. (2008). Calculating wave-generated bottom orbital velocities from surface-wave parameters. Computers & Geosciences 34, 1243–1262.

WMO (1998). Guide to wave analysis and forecasting. World Meteorological Organization 702, Geneva, 159 pp.

Wright, L.D. (1995). Morphodynamics of Inner Continental Shelves. CRC Press, Boca Raton, 241pp.